STOCKHOLM UNIVERSITY

DEPARTMENT OF PHYSICS

EXANA, a program for analysing
EXtended Energy Loss Fine Structures,
EXELFS spectra

M.A. Tafreshi, C. Bohm and S. Csillag

USIP Report 92- 01 September 1992

EXANA, a program for analysing EXtended Energy Loss Fine Structures, EXELFS spectra

M. A. Tafreshi, C. Bohm, and S. Csillag

Institute of Physics, University of Stockholm
Vanadisvägen 9, S-113 46
Stockholm

ABSTRACT

This paper is a users guide and reference manual for the EXANA, an IBM or IBM compatible PC-based program used for analysing extended fine structures occurring on the high energy side of the ionisation edges. The RDF (Radial Distance Function) obtained from this analysis contains information about the number, distance, and type of the nearby atoms, as well as the inelastic mean free path and disorder in distances from the centre atom to the atoms in a atomic shell around it. The program can be made available on request.

CONTENTS

1. INTRODUCTION

Because of the sensitivity to the nearby environment, analysis of the Energy Loss Fine Structure can provide a great deal of structural information about the nearby atomic environment around a particular type of atom.

This report apart from being a review of the EXELFS phenomena and the physics behind different steps in the analysis, is a user and reference manual for analysing EXELFS spectra with the EXANA program. To visualise the analysis sequence, analysis of a spectrum from a relatively thick region of a graphite sample (see figure 1) has been illustrated step by step.

2. THE EXANA PROGRAM

Running the program requires an IBM or IBM compatible PC computer with enhanced graphics. User interface of the EXANA is based on "pull down" menus that are activated by the mouse. All commands can be given from these menus. A menu bar, from which the different "pull down" menus are activated, is situated at the top of the screen.

A menu is activated by pointing at the menu bar, and pressing the left mouse button. As long as the mouse button is kept down, the selected menu stays on the screen. Each menu contains a list of commands that can be selected by pointing the cursor. When the mouse button is released, the selected command is activated and the menu disappears.

On-line help is available all the time by pressing, and holding down, the right mouse button when an item in a menu is selected. The help information stays on the screen until the right button is released. It is thus possible to check the action performed by a command before the command is executed.

The menus used in the program are **File**, **Display**, **Calculation**, and **Help**. Following contains a short description of each of the commands used in these menus.

2.1. File commands. — The commands in this menue are dealing with the file managing. These commands are:

Number of points. – This command can be used to change the number of data points from 512 to 256 or vice versa. The default value is 512.

Path. – Path specifier the directory from where data files can be loaded. The default path is the path to the current directory.

Load EXELFS. – To load the EXELFS data file (figure 1a). Number of loaded data points can be 512 or 256 depending on the value chosen with the "Number of points".

Load Low-loss. – This command loads the low-loss spectrum (figure 1b). When loading low-loss or EXELFS spectrum, the program ignores the first three rows of the data file, and reads only data from the fourth row, i.e. the first three rows in the data file can be used for storing comments.

Write to. – This command saves the current displayed spectrum in a file.

Exit (ESC). – This command leaves the program. It can also be activated by pressing the <Esc> key.

2.2. Display commands. — These commands are used to display the data during the analysis. These commands are:

EXELFS Rawdata. – Displays the raw EXELFS data (figure 1a).

Low-Loss data. – In this the low-loss data, containing the energy losses due to the zero-loss and plasmon excitation are displayed (figure 1b).

Pre-edge BSub. – Here the data after pre-edge background subtraction is shown.

Data & Backgr. – This command displays raw data together with corresponding pre-edge background.

Gaussian Fun. – Displays the Gaussian function which will be used in the deconvolution procedure.

Deconvoluted. – This command shows the deconvoluted data.

Main BSub. – Here the data after main background subtraction is shown.

Data & Backgr. – The data before main background subtraction together with the corresponding fitted background is displayed.

Chosen Interv. – Shows the data interval chosen for further analysis.

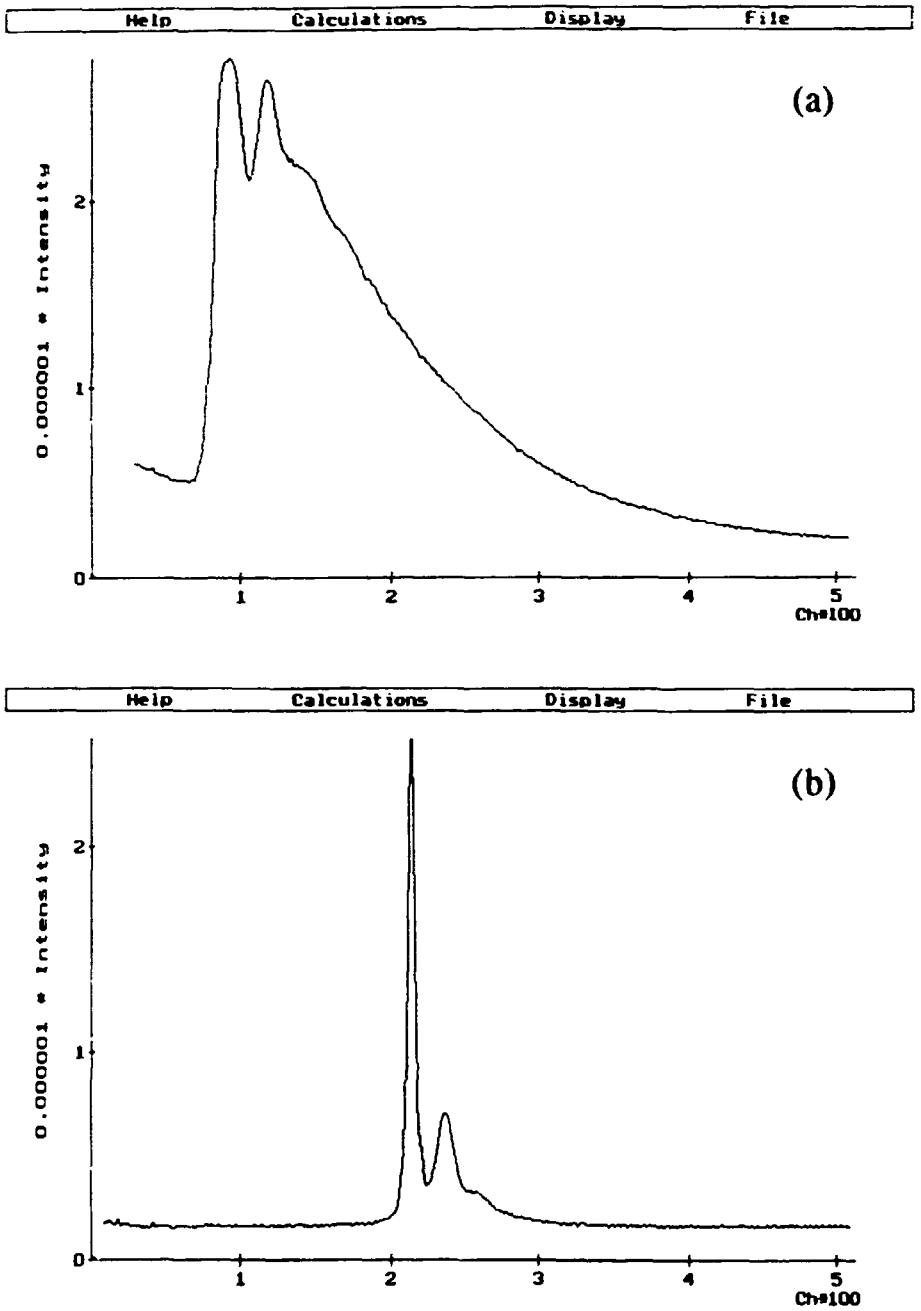

Fig. 1. — (a) is the energy-loss spectrum of a relatively thick region of a graphite sample. (b) displays corresponding low-loss spectrum.

Converted data. – Displays the data after conversion from energy space to k-space.

K-corrected. – The data after compensation for k-dependent factors, and multiplication by the window function, displays.

Mag. of FFT. – Displays the magnitude of the Fourier transformed data (i.e., the Radial Distance Function or RDF).

Phase-Shift. – This command displays phase-shift spectrum obtained from the real and imaginary parts of the Fourier transform.

Real & Image. – Displays the Real and Imaginary parts of the Fourier transform.

Real Part. – Here the real part of the Fourier transform is shown.

Imaginary Part. – This command shows the imaginary part of the Fourier transform.

2.3 Calculation commands. — The commands in this menu perform the calculations. While chapter 5 contains the physics behind these calculations, and the possible errors introduced by them, chapter 6 contains a description of how these commands can be performed. However a short presentation of these commands and their function are given in the following:

PBsub. – To calculate and remove the pre-edge background.

Low-Loss. – To find the value of eV per channel, prepare the low-loss spectrum for deconvolution, and generate a Gaussian function.

Deconvolution. – Performs the deconvolution of the low-loss from the EXELFS spectrum, by using the Gaussian function as the filter function.

Thres. Pos. – To choose the energy threshold position.

BSub. – Isolates the oscillatory part of the data by subtraction of the main background.

Range. – To choose a suitable range of the data for further analysis.

Conversion. – Converts the data from energy space to k-space.

K-Correction. – To compensate data for decreasing effect of the k-dependent factors, and multiplication by the filter function.

FFT. – Performs a fast Fourier transform of the data.

Phase & Dist. – Calculates φ_0 (see chapter 4.9) for a particular peak, and displays it together with the corresponding distance.

2.4 Help. — This is not an ordinary menu. When selected, a message window is shown with some general information about the program. Help on a specific command is available all the time by pressing the right mouse button while the command is selected.

3. A REVIEW OF THE EXELFS PHENOMENA

The energy distribution of electrons passing through a thin foil of material is a direct measure of the electronic excitations produced in the sample by the electron beam. During inelastic scatter events, the incident electrons can produce inner-shell ionisations and hence the atom becomes ionised.

A part of the outgoing ejected electron wave is being backscattered from the surrounding atoms. This backscattered wave can interfere with the outgoing part of the ejected electron wave and thereby affects the probability of ionisation[1], which can be interpreted as the probability for a certain energy loss being increased or decreased, depending on the circumstances in the local atomic environment in the sample. This effect is observed as the modulation occurring on the high energy side of the ionisation edges, extending from a few eV to a few hundred eV above the edge and is called Energy Loss Fine Structure.

The Energy Loss Fine Structure can be separated into two regions, the near-edge structure, which ranges about 5-10 to 15-50 eV of the edge, and the EXELFS (i.e., EXtended Energy Loss Fine Structure), which extends from 15-50 eV up to a few hundred eV.

The near-edge structure is known to be sensitive to both the local arrangement of atoms around the absorbing atom as well as the atomic states of the absorbing atom[2]. The EXELFS, on the other hand, is "only" sensitive to the arrangement of atoms around the absorbing atom which

can be interpreted in terms of backscattering of the ejected core electron wave by atoms around the excited atom.

By approximating the ejected electron wave function at the backscattering atom site with a plane-wave while assuming single-scattering and single electron formalism with small scattering angles, the modulations can be described[3] by:

$$\chi(k)=\sum_j \frac{N_j}{r_j^2}\cdot\left(\frac{f_j(k)}{k}\cdot e^{-2\cdot\sigma_j^2\cdot k^2}\cdot e^{-2\cdot r_j/\lambda_i}\right)\cdot\sin(2kr_j+\Phi_j(k)) \qquad (1)$$

where k is the wave number of the ejected electron, N_j is the number of atoms in shell j, r_j is the radius, $\Phi_j(k)$ is the phase change of the electron wave after travelling through the potential of the emitting and backscattering atoms, $f_j(k)$ is the backscattering amplitude which depends on the type of backscattering atoms, λ_i is the mean free path for inelastic scattering of the ejected electron, and σ_j is a parameter describing the distribution of the interatomic distances due to structural disorders. Depending on what is considered known parameters, this expression can provide means for deriving additional information [i.e., r_j, N_j, λ_i, $\Phi_j(k)$, $f_j(k)$, and σ_j] about the local environment of the excited atom.

4. THE PHYSICS BEHIND THE ANALYSIS PROCEDURES

The following is a description of the physics behind different analysis steps[4-6], with a review of eventually errors introduced by these steps.

4.1 Pre-edge background subtraction. — This step in the analysis is primarily concerned with removing other absorption effects than those related to the edge under study. Inner-shell ionisation edges are mostly superimposed upon monotonically decreasing backgrounds which originate from the excitation of atomic electrons with lower binding energy. After approximating this background with an appropriately decreasing function, it can be removed from the spectrum. This is done by fitting a smooth function to the data below the edge, extrapolating it into the core-loss region and subtracting it from the measured data.

In order to minimise the truncation effects after deconvolution. it is desirable that this background asymptotically approaches the high energy side of the spectrum.

4.2 Calibration of the energy-loss axis. — The next step is to compare an independently determined plasmon or inner-shell excitation energy with the distance measured in channels, between the first (zero-loss) and the second peak (energy-loss due to plasmon or inner-shell excitation) in order to calibrate the energy-loss axis.

The calibration of the energy axis has a direct effect on the result of the analysis. An inaccurate calibration of the energy-axis introduces a constant relative error in k and in the interatomic distance r, which for small deviations in E_{ref}, should be:

$$\frac{\Delta r}{r} = -\frac{\Delta E_{ref}}{2 \cdot E_{ref}} \tag{4}$$

4.3 Removal of the plural scattering contribution. — The contribution from the plural scattering may have to be removed before the extended fine structure can be interpreted, particularly in the case of relatively thick samples.

Plural scattering[7] occurs when an electron suffers one or more inelastic excitations (outer-shell excitation) in combination with the core-loss ionisation. Since the probability of these excitations increase with increasing sample thickness, the thickness of the examined sample region can drastically alter the observed shape of the modulations. It will also decrease the signal to background ratio, which in turn degrades the statistics.

The plural scattering causes a shift in the associated EXELFS-spectrum. To a first order, plural scattering will affect the EXELFS spectrum in the same way as incident electrons with an energy distribution shaped like the low-loss distribution, where the low-loss region can be defined as the region corresponding to energy-losses below 100 eV. This region contains the zero-loss energy and energy-losses due to plural scattering (see figure 1b).

The probability for an electron to be inelastically scattered n-times while passing through a sample of thickness t, is given by[7,8]:

$$P_n = \frac{1}{n!} \cdot \left(\frac{t}{\lambda_{in}}\right)^n \cdot \exp\left(-\frac{t}{\lambda_{in}}\right) \tag{2}$$

where t/λ_{in}, is the mean number of collisions within the specimen, and λ_{in} the mean distance between collisions, known as the mean free path for inelastic scattering (Observe that the λ_{in} here differs from the λ_i in expression 1). In the case of very thin samples, the low-loss region mainly consists of unscattered electrons (zero-loss) that have not lost kinetic energy in the sample. In this case the energy distribution is due to the energy distribution from the electron source.

Experimentally, the ratio between local thickness of the sample, and the inelastic mean free path λ_{in}, can be estimated from the following expression:

$$\frac{t}{\lambda_{in}} \cong \ln\left(\frac{I_{tot}}{I_0}\right) \tag{3}$$

where I_{tot} is the total intensity in the spectrum, and I_0 is the integrated intensity under zero-loss peak.

Inserting the experimentally obtained value for t/λ_{in} in to the equation (2), the probability for inelastic scattering can be calculated.

The expression 2 shows that plural scattering becomes appreciable if the specimen thickness approaches the inelastic mean free path. For example, for $t=\lambda_{in}$, expression 1 leads to $P_0=P_1=0.37$, $P_2=0.18$ and $P_3=0.06$. Under these circumstances the effect of plural scattering on the analysis should be considered.

However, a complete deconvolution is, in practice, impossible because in addition to removing the plural scattering contribution, the deconvolution also removes the influence of the system resolution function. The resolution is thus improved but at the expense of greatly amplified noise. It is therefore necessary to apply a filter function to smooth the deconvoluted data before continuing analysis. In practice this can be performed by a convolution between the deconvoluted data and a function which can replace the resolution function.

Since the deconvolution process is very sensitive to the defects and artefacts in the data, a successful removal of plural scattering effects by deconvolution requires accurate spectra.

4.4 Identification of the energy threshold position. — The energy threshold position should be identified as the origin of the energy axis.

An inaccurate choice of the edge position causes an inaccuracy in the energy axis which in turn leads to a nonlinear deformation of the k-axis. This may be regarded as stretching and translating the interval to adapt to the kmin and kmax values followed by a non-linear deformation of the spectrum within the analysing interval.

Practically, the selection of the threshold position to the right (towards higher energies) of its real position will result in a reduction of the measured interatomic distances (and vice versa) with broadened peaks due to the non-linear effects.

For small deviations in the edge position, the deviation in wave number of a particular channel can be described by

$$\frac{\Delta k_i}{k_i} = -\frac{1}{2}\frac{\Delta p}{i-p} \tag{5}$$

where i is the channel number, k_i is the wave number of channel i, p is the channel number of the real edge position, and Δp is the deviation in the chosen edge position from the real position.

This expression indicates that the effect of an inaccurate edge position decreases significantly with an increasing distance from the edge, which means that, the errors can be minimised by choosing the analysing interval as far above the edge as possible.

A closer examination of eq. (5) reveals that it is more adequate to choose the edge position above the real edge rather than below it; e.g., if edge position is chosen 5 channels below the real edge and E_{min} 30 channels above the chosen edge, then there is –10% deviation in k_{min} value. Choosing, instead, the edge position 5 channels above the real position, the deviation in the k_{min} value will decrease to +7%.

4.5 The main background subtraction. — The oscillatory part of the core-loss intensity $\chi(E)$ is obtained by normalising the measured intensity J(E) to the intensity corresponding to the single isolated atom case A(E), i.e. the intensity which would have been measured if neighbouring atoms were absent (see expression 7).

$$\chi(E) = \frac{J(E)}{A(E)} - 1 \tag{6}$$

In general A(E), is not directly available experimentally and can not be theoretically calculated with sufficient accuracy. An empirical approximation can, however, be obtained by fitting a polynomial function or a continuous combination of polynomials through J(E). The fact that the background should correctly follow the overall trend of the data but not the EXELFS modulations themselves (otherwise false structure will appear in RDF at small values), requires use of low-order polynomials and not too short branches.

4.6 Scale conversion. — The interference amplitude, initially presented as a function of energy, is now converted into a momentum representation. In this representation the interference amplitude can be decomposed into sinusoidal components corresponding to reflections from different neighbouring atoms.

Since the velocity of the ejected electron is low compared to the speed of the light, the wave vector k of the ejected electron can be determined using classical mechanics. If energies are measured in eV and k in nm^{-1}, the formula becomes:

$$k=5.123\sqrt{E_{kin}}=5.123\cdot(E-E_0)^{1/2} \qquad (7)$$

where E_{kin} is the kinetic energy of the ejected electron, E is the energy transferred from the incident electron to the ejected core electron, and E_0 is the energy required for the core electron to become free (i.e., energy loss corresponding to the threshold position).

4.7 Preparing for Fourier transform. — Before attempting to Fourier transform a compensation for the decaying effect of the k-dependent factors [i.e. 1/k, $f_j(k)$ and the σ-term, see expression 1], of the modulations should be performed. This is usually achieved by multiplying the data with k^n where k is the wave number of the ejected electron and n is a number between 1 and 3. The actual choice of n depends on the rate at which $\chi(k)$ decreases (which in turn depends on the backscattering amplitude of the neighbouring atoms) as well as the noise level.

The data should also be multiplied by a window function to minimise the effect of truncation after the Fourier transformation.

The fact that the typical data intervals available for FFT usually are short compared to the wavelengths of the principal modulations, implies that the interesting part of the Fourier transform is sparsely sampled. A

zero-extension of the data before the Fourier transform will improve the sampling. However, the effect of this operation is mainly to perform an appropriate interpolation between the original sample points.

Another adjustment made before the Fourier transformation is the addition of a constant level in order to remove the zero frequency component.

4.8 Fourier transformation. — Fourier transform of the $\chi(k)$ yields the RDF (i.e., magnitude of the Fourier transform).

While the position of the peaks in the RDF depends on the combined effect of the phase shift $\Phi j(k)$, and interatomic distances rj, the intensity of the peaks depends mainly on the number of atoms in a particular shell Nj, and the mean free path of the ejected electron λ_j.

The width of the peaks depends mainly on the length of the analysing k-interval, but is also affected by an insufficient compensation for the k-dependence, by the window function, and by errors in the position of the threshold-energy.

The phase shift corresponding to a particular peak, obtained from the imaginary and real part of the FFT, is the phase shift of the corresponding wave at the k_{min}.

4.9 Phase shift correction. — Throughout it's journey, the ejected electron experiences the phase shift (Coulombic interaction) of the absorber atom twice (i.e., once going out and once coming back) and the phase shift of the scatterer once.

The total phase shift (see expression 1) $\Phi_j(k)$, for K-shell ionisation edges is described by:

$$\Phi_j(k)+\pi=\Phi_a(k)+\Phi_b(k) \qquad (8)$$

where $\Phi_a(k)$ and $\Phi_b(k)$ are phase shifts due to the central respectively backscattering atoms. These phase shifts have been calculated and tabulated by Teo & Lee[9], and by McKale et al.[10,11].

For many elements the total phase shift $\Phi_j(k)$, is approximately linear in k over the analysing interval and can be written as:

$$\Phi_j(k)+\pi=\varphi_0+\varphi_1 \cdot k \qquad (9)$$

While φ_0 is a constant phase term which can not affect the distances obtained from the RDF, φ_1 introduces a shift of these distances towards lower values. For those elements for which $\Phi_j(k)+\pi$ can not accurately be described by eq. 3, this expression is still a linear approximation to it.

A comparison between expression 9 and 1 implies that the experimental distance obtained from the RDF is equal to $r+\varphi_1/2$. Thus an a priori knowledge about φ_1 allows the determination of the interatomic distance, while known interatomic distance φ_1.

The imaginary and real part of the Fourier transform yields the phase shift corresponding to a particular peak at k_{min} (in the k-space). Using this phase and the corresponding frequency allows the determination of the value of $\varphi_0-\pi$ and φ_0 for a particular peak.

5. ANALYSING WITH EXANA

After loading the EXELFS and low-loss data files through the **File** menu, by using commands from the **Calculation** menu, analysis proceeds as follows:

5.1 PBsub. — The two following functions for the calculation of the pre-edge background are available:

$$F(i)=A+\frac{B}{i+C} \tag{11}$$

$$F(i)=A+B\cdot i^{-1}+C\cdot i^{-2} \tag{12}$$

where A corresponds to an energy independent part of the background, B and C are free parameters and i is the channel number. After A has been chosen as the estimated constant background level, B and C are determined by least square fitting of F to the pre-edge region. If no direct measurements of the constant background are available, a reasonable estimate can be made by choosing a fraction of the value corresponding to the largest energy loss as the constant background.

After choosing the PBSub, and by typing the corresponding number, one of the four following commands can be chosen.

1- *Exponential function.*

2- *Polynomial function.*

3- *Least square fit to exp. function.*

4- Least square fit to pol. function.

By using the mouse, three position of the spectrum should be selected, where the two first points are to identify the fitting pre-edge region, and the third marks the position of a point with known intensity at the end part of the spectrum. After choosing these three points, the program asks for the intensity factor. The intensity corresponding to the third point is then multiplied by this value to determine the constant level.

In all four cases above, the selected points are used to solve the chosen equation (i.e. 11 or 12). The values of A, B, and C are presented as the default values. It is possible for the operator to change the default values. The values used for A, B, and C, are written in a file named as MINP.OUT.

After subtraction of the pre-edge background, the first data point of the interval of interest must be identified by the operator. This is to remove the non interesting part (i.e., the pre-edge region) of the data.

If performation of the deconvolution procedure is not intended, this command (i.e., **PBSub**) can be ignored.

Figure 1a shows a spectrum from a relatively thick region of a graphite sample. The low-loss part of this spectrum is in figure 1b. Figure 2a displays the data from figure 1a, with corresponding pre-edge background. Figure 2b is the same after pre-edge background subtraction.

5.2 Low-Loss. — To determine the eV per channel, the program asks whether the eV/Ch is known or not. If it is known previously, then the value of eV/Ch should be typed, otherwise the program asks after the plasmon excitation energy. This energy and the channel distance between the zero-loss and first plasmon top, are used to calculate the value of eV per channel.

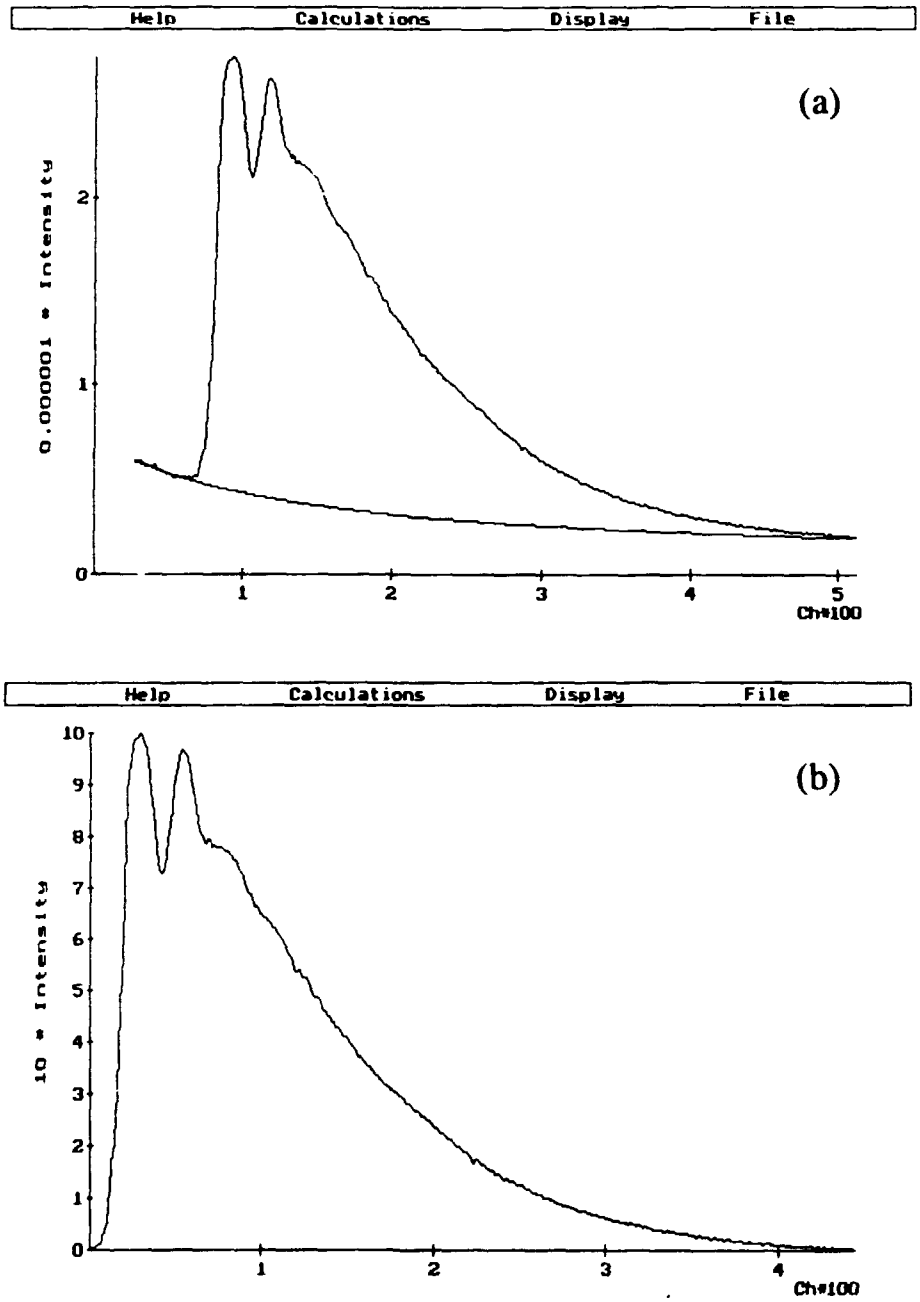

Fig. 2. — (a) shows the data from figure 1a, but with a pre-edge background inserted. (b) is the same data after pre-edge background subtraction.

To remove the non interesting part of the low-loss spectrum and to prepare the data for deconvolution, a point of the low-loss spectrum should be identified as the beginning point of the spectrum. The intensity corresponding to this point, is subtracted from all other intensities. Intensities before this point, and all negative intensities are set to zero. Figure 3a shows the low-loss in figure 1b after this step.

A narrow Gaussian function is also generated with a standard deviation determined by the operator. Figure 3b displays the Gaussian function used in the analysis procedure in this work.

5.3 Deconvolution. — A Fourier transform based deconvolution technique is used, performing a complex division between the Fourier transform of the core-loss region and the Fourier transform of the low-loss region.

The Gaussian function generated in the previous step, is used as the filter function. Choosing the width of the Gaussian is a trade off between too much noise if the width is too small and deteriorated resolution if the width is too large. In practice ,in order to find the optimum width, the deconvolution procedure has to be repeatedoften with different Gaussian functions. However, the width of the zero-loss peak provides a good starting value.

Figure 4a shows spectrum in figure 2b after deconvolution with spectrum in figure 3a and convolution with spectrum in 3b.

If deconvolution is not necessary, this command can be ignored.

5.4 Thres. Pos. — Selection of an appropriate threshold-energy position has been recognised as an important but difficult problem, which must be confronted when performing EXELFS-type analysis.

There are some suggestions[12,13] for proper determination of this position (in the literature referred to as the E_0 problem), but non of them can be regarded as the definite method.

In the analysis of a NiO sample, by a comparison between the near-edge part of the experimental spectrum and the theoretically calculated near-edge structure, this position could be identified with an accuracy of about ±0.25 eV, which is sufficient for this kind of analysis. However, the effect of the inaccuracy due to this step can be predicted by analysing simulated data, simulated under the same conditions as the experimental one.

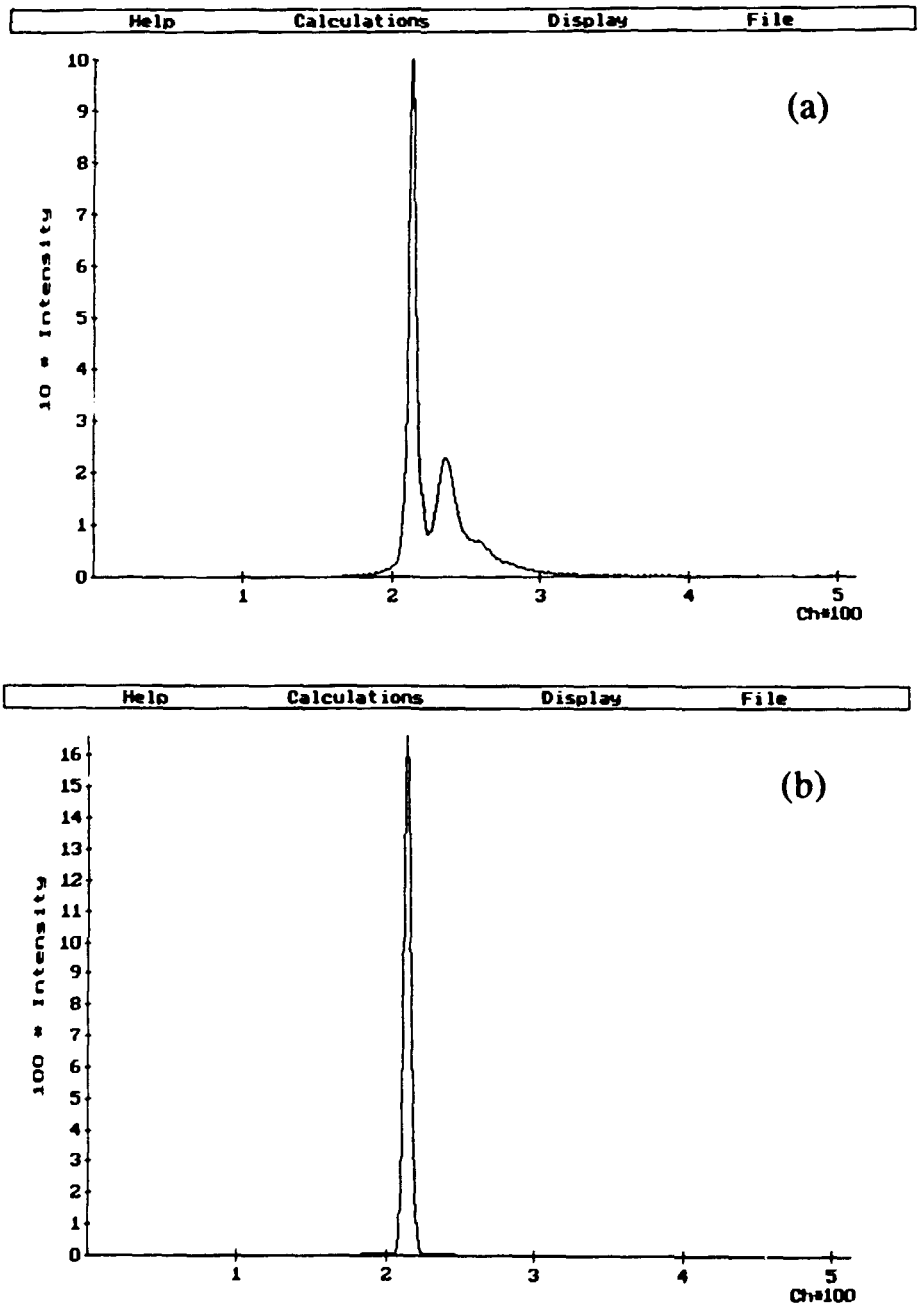

Fig. 3. — (a) displays the low-loss spectrum in figure 1b, after removing a constant intensity. (b) shows the Gaussian function used as the new resolution function when deconvoluting the spectrum in figure 2b.

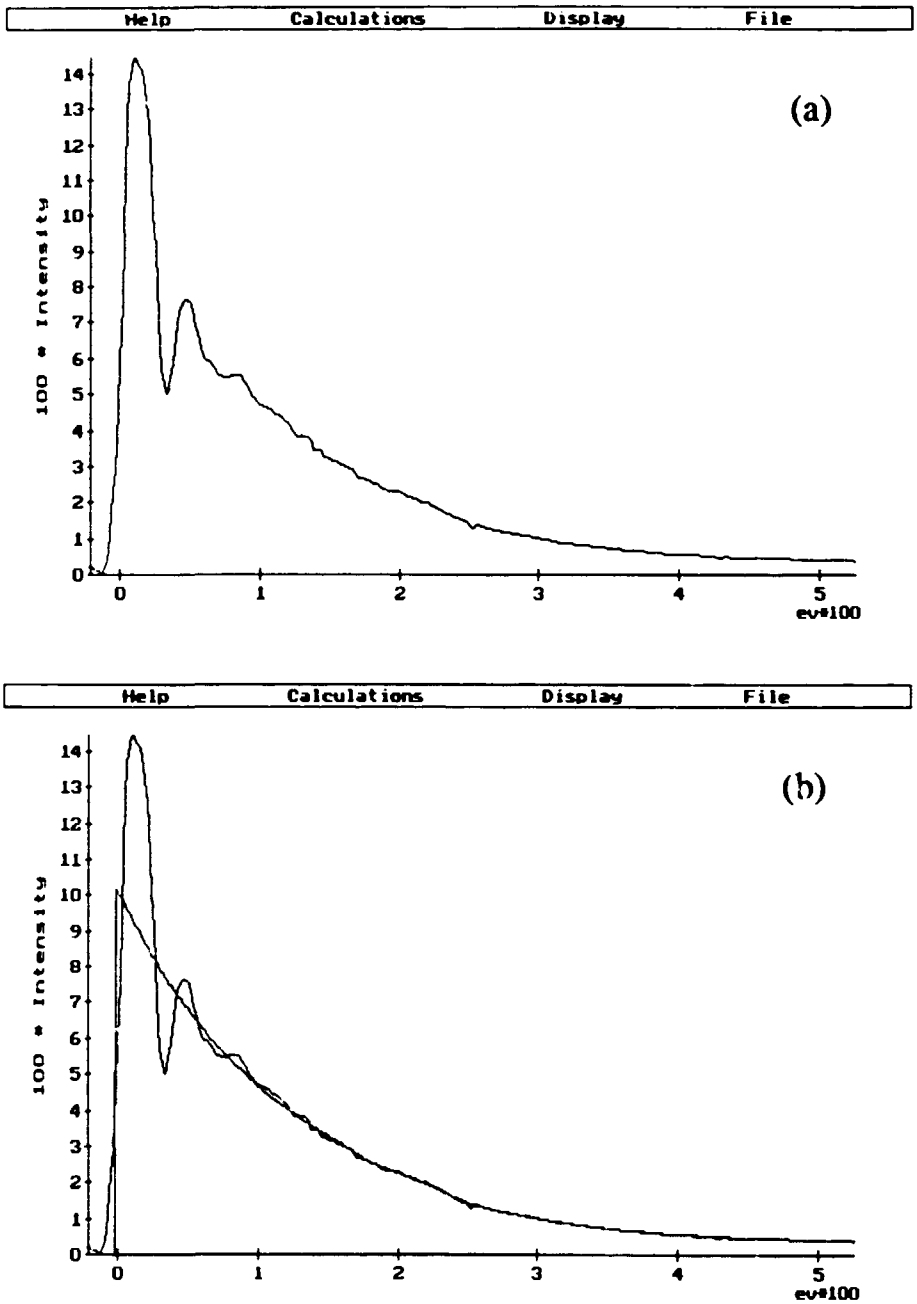

Fig. 4. — (a) is the spectrum from figure 2b after deconvolution with the low-loss spectrum from figure 3a, and convolution with the Gassian function from figure 3b. (b) displays the deconcoluted data with corresponding background.

At this point, the data reflects the energy distribution of the emitted electron wave, which may be assumed to be a smooth function of the energy, augmented by interference effects caused by the reflected wave. The smooth function corresponds to the intensity which would have been measured in the absence of neighbouring atoms (i.e., the free atom energy distribution).

5.5 BSub. — This step is performed by fitting one or a few third order polynomial functions to different parts of the data. Since when activating this command only one fitting to one region of the data is performed, to form a background composed of different parts, this command has to be activated a few times.

After calculating a background of a partition, it is possible to save all or a part of it.

The deconvoluted data in figure 4a, together with the corresponding polynomial background, is shown in figure 4b. This background consist of three partitions of a third order polynomial. The interesting region of the obtained oscillatory part is displayed in figure 5a.

5.6 Range. — In this step the interesting part of the data interval can be chosen for further analysis.

To avoid influence from the near-edge effects and to reduce the sensitivity to deviations in the selection of threshold-energy position, the start point of the analysing interval should be chosen at about 25 eV (26 nm^{-1}). The end point of the interval should be chosen to maximise the information content, since beyond a certain point, increase of the interval will mainly increase the noise.

However, the multiplication by a window function (see below) before the Fourier transform introduces strong damping at the beginning and the end of the analysing interval, reducing its effective length. This unintended reduction may be compensated by extending the data interval below and above the prior end points.

The short data interval and the presence of noise introduces errors in the determination of interatomic distances (i.e. of the peak positions in the RDF). The deviations can vary from zero to a few percent. Therefore, it is often advisable to average results from the analysis with different intervals to improve reliability.

5.7 Conversion. — Further analysis requires resampling of the data so that it becomes equally spaced in electron wave-number space, i.e. a scale conversion from $\chi(E)$ to $\chi(k)$ followed by some interpolation in the k-space must be performed. While a change of the scale is obtained by using equation 7, a linear interpolation is used to obtain the equally spaced data after conversion.

After this step, the interference amplitudes can be regarded as "pure" EXELFS modulations, i.e. they can be described by the expression 1.

5.8 K-Correction. — To compensate for the damping effect of the k-dependence factors, it is possible here to multiply the data with k^n where k is the wave number of the ejected electron and n is a number between 1 and 3. The data can also be multiplied by a filter function, which varies as $\cos^2_i$ at the ends of the data range but is flat over 50% of the central region.

Figure 5b displays the data in figure 5a after conversion from energy to k-space, multiplication by k^2 and the filter function.

5.9 FFT. — In practice, a fast Fourier transform (FFT) procedure is used and the radial distribution function (RDF) of neighbouring atoms is obtained as the magnitude spectrum of this transform. For an accurate EXELFS analysis, the effect of low resolution and truncation artefacts should also be considered. More accurate results can be obtained by fitting the RDF from a simulated spectrum, corresponding to the same conditions as the experimental, to the RDF of the experimental data. This can be performed by using an simulating program named SIMANA.

The RDF of the non deconvoluted data corresponding to the spectrum in figure 2b is shown in figure 6a. Figure 6b shows the RDF corresponding to the deconvoluted data in figure 5b. Detailed information about the result of this analysis can be obtained from the already published paper[5].

5.9 Phase & Dist. — The imaginary and real part of the Fourier transform yields the phase shift corresponding to a particular peak at k_{min} (in the k-space). With this command a peak in the magnitude spectrum of the Fourier transform can be selected. By calculating the corresponding phase at the k_{min}, and extrapolating the frequency corresponding to this peak from k_{min} to k_0 (or E_0), the program determines the value of $\varphi_0-\pi$ (see chapter 4.9) for a particular peak.

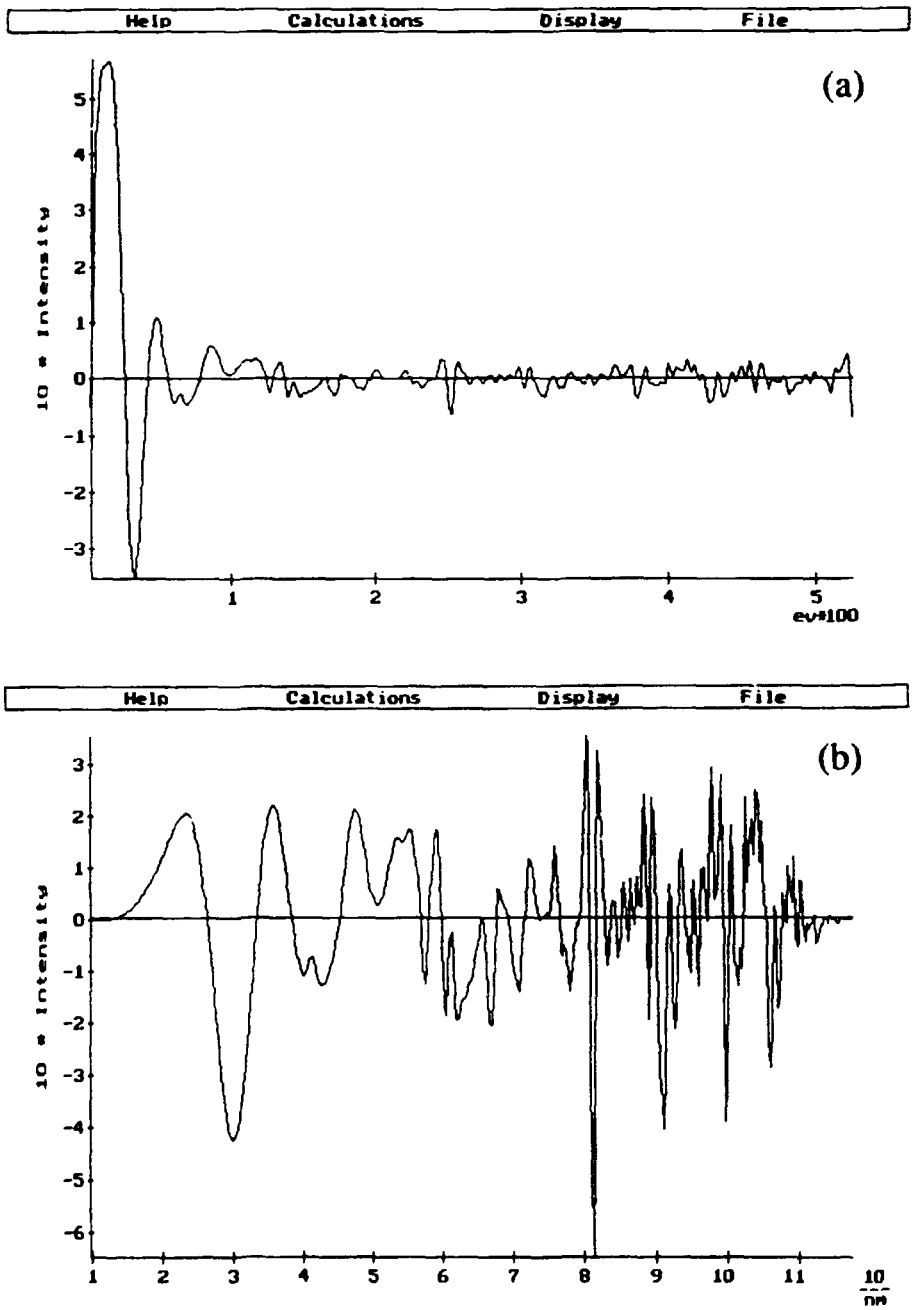

Fig. 5. — (a) is the selected part of the background subtracted data, and (b) is spectrum from (a) after conversion from energy space to k-space, multiplication by k^2 and filter function.

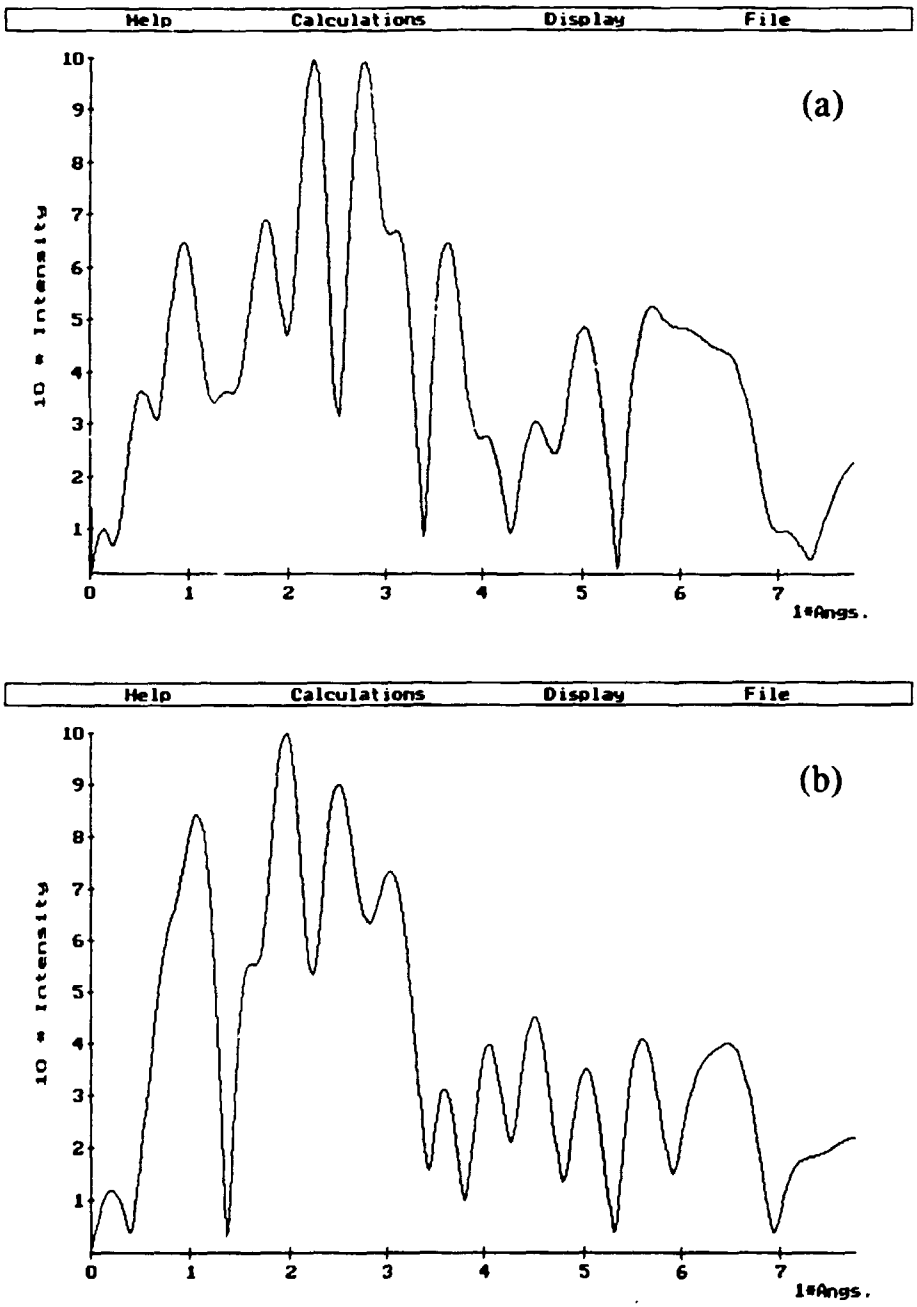

Fig. 6. — (a) shows the RDF obtained from the analysis of the non deconvoluted data. (b) is the RDF of the modulations in figures 5b, i.e. of the deconvoluted data.

REFERENCES

1. R. de L. Kronig, Zeit. f. Physik **75**, 468 (1932).
2. David A. McKeown, Phy. Rev. **B45**, 2648 (1992).
3. E. A. Stern, Phys. Rev. **B10**, 3027 (1974).
4. M. A. Tafreshi, Ch. Bohm, and S. Csillag, Microsc. Microanal. Microstruct. **1**, 199 (1990).
5. M. A. Tafreshi, S. Csillag, Z. W. Yuan, and C. Bohm, Microsc. Microanal. Microstruct. **2**, 515 (1991).
6. M. A Tafreshi, S. Csillag, Z. Yuan, C. Bohm, E. Lefèvre, and C. Colliex, Inelastic mean free path and phase-shift determinations in NiO, submitted for publication to JOURNAL DE PHYSIQUE, 1992.
7. R. F. Egerton, Electron Energy-Loss Spectroscopy in the Electron Microscope.
8. R. D. Leapman, and C. R. Swyt, Analytical Electron Microscopy 1981, ed. R. H. Geiss, San Francisco Press, San Franciso, P.g. 164-172.
9. Teo B.-K., and Lee P. A. Ab initio calculations of amplitude and phase functions for extended x-ray absorption fine structure spectroscopy, J. Am. Chem. Soc. **101**, 2815 (1979).
10. A. G. McKale, G. S. Knapp, and S.-K. Chan, Phy. Rev. **B33**, 841 (1986).
11. A. G. McKale, B. W. Veal, A. P. Paulikas, S.-K- Chan, and G. S. Knapp, J. Am. Chem. Soc. **110**, 3763, (1988).
12. P. A. Lee, and G. Beni, Phy. Rev. **B15**, 2862 (1977).
13. David V. Baxter, EXAFS and Near Edge Structure III, edited by K. O. Hodgson, B. Hedman, and J. E. Penner-Hahn, ISBN: 3-540-15013-7, 1984, P.g. 77.